Materials Letters 212 (2018) 346–349

Contents lists available at ScienceDirect

Materials Letters

journal homepage: www.elsevier.com/locate/mlblue

Selective laser melting of a Ti-based bulk metallic glass

Liang Deng [a], Shenghai Wang [b], Pei Wang [a], Uta Kühn [a], Simon Pauly [a,*]

[a] Institute for Complex Materials, IFW Dresden, Helmholtzstraße 20, D-01069 Dresden, Germany
[b] School of Mechanical, Electrical & Information Engineering, Shandong University (Weihai), Wenhua Xilu 180, 264209 Weihai, PR China

ARTICLE INFO

Article history:
Received 22 September 2017
Received in revised form 20 October 2017
Accepted 31 October 2017
Available online 31 October 2017

Keywords:
Selective laser melting
Ti-based alloy
Bulk metallic glasses
Biomedical applications
Mechanical properties

ABSTRACT

The Ti-based bulk metallic glass $Ti_{47}Cu_{38}Zr_{7.5}Fe_{2.5}Sn_2Si_1Ag_2$ was fabricated by selective laser melting (SLM). The crystalline phases in the gas-atomized powder disappear after additive manufacturing and the SLM parts are fully glassy. All SLM samples reach a high relative density above 98.5% and a high compressive strength around 1700 MPa despite failing prematurely in comparison with as-cast rods. Our work identifies a Ti-based glass-forming alloy suitable for laser-based additive manufacturing and opens up new vistas for overcoming the intrinsic limitations of Ti-based BMGs in terms of size and geometry and for making them accessible to (biomedical) applications.

1. Introduction

Bulk metallic glasses (BMGs) have attracted increased attention as biomaterial [1,2] because of their unique combination of properties, unmatched by most conventional alloys [3]. BMGs generally exhibit high yield strength, low wear rates, relatively low Young's moduli and good fatigue resistance [4]. These advantageous physical properties result in a high load-bearing capability and can reduce stress-shielding or the generation of wear debris, which is crucial when being used as implants [5,6]. Due to their bioinertness titanium and its alloys have already been used in the biomedical sector for decades and also additively manufactured components have been investigated for this field of application [5,7–9]. Therefore, it appears natural to investigate the applicability of Ti-based BMGs as biomaterials in order to exploit their unique properties [2]. However, only when the toxic element Be is present does the critical casting thickness of Ti-based alloys reach relatively high values (above 50 mm in Ti-Zr-Cu-Ni-Be) [10]. The inherently low glass-forming ability (GFA) combined with poor machinability represents a major obstacle for most applications.

New processing technologies could help to overcome these problems. Selective laser melting (SLM) [11] bears great potential for producing large-scale as well as glassy components with an almost unlimited freedom regarding the design. Therefore, SLM has been increasingly applied to various glass-forming alloys, such as Fe-based [12,13], Al-based [14] and Zr-based systems [14–16]. Additively manufactured Ti-based BMGs, however, do not exist so far even though they could be of high interest for a wide variety of applications even beyond biomedical applications.

In this study, the biocompatible glass $Ti_{47}Cu_{38}Zr_{7.5}Fe_{2.5}Sn_2Si_1Ag_2$ (at.%) [17] was fabricated via SLM. We assess its suitability for selective laser melting and investigate the effect of the processing route on the phase formation, the relative density and the deformation behaviour.

2. Experimental procedure

$Ti_{47}Cu_{38}Zr_{7.5}Fe_{2.5}Sn_2Si_1Ag_2$ ingots were gas-atomized by Nanoval GmbH and a particle size between 10 and 90 μm was used. Rods with a diameter of 2 mm were prepared by suction casting. The SLM samples were produced in a SLM 50 (Realizer GmbH) with a laser power of 60 W, a scanning speed of 2000 mm/s, a hatch distance of 140 μm and a layer thickness of 40 μm. Unidirectional scanning vectors were used and rotated by 90° in adjacent layers. The chemical composition and oxygen content of the powder and the SLM parts were measured using inductively-coupled plasma optical emission spectroscopy (Thermo Fischer Scientific) and carrier gas hot extraction (LECO), respectively. X-ray diffraction (XRD) was done on a D3290 PANalytical X'pert PRO diffractometer with Co-K_α radiation ($\lambda = 0.17889$ nm). Differential scanning calorimetry (DSC) was conducted in a Perkin-Elmer Diamond (heating rate of 0.33 K/s). X-ray computed tomography (μ-CT) was performed with a Phoenix nanotom m (General Electric) at 130 kV and 100 μA and with a voxel size of about

* Corresponding author.
E-mail address: s.pauly@ifw-dresden.de (S. Pauly).

https://doi.org/10.1016/j.matlet.2017.10.130
0167-577X/

5 μm. The relative densities were additionally evaluated by the Archimedean principle. Room-temperature compression tests were carried out at a strain rate of 2×10^{-4} s^{-1} using an Instron 5869 for at least three specimens (diameter: 2 mm, height: 4 mm). Scanning electron microscopy (SEM, Gemini 1530, Carl Zeiss AG) was employed to investigate the fracture morphologies of the broken specimens.

3. Results and discussion

The actual composition of the gas-atomized powder, $Ti_{46.9}Cu_{38.13}Zr_{7.43}Fe_{2.52}Sn_{2.02}Si_1Ag_2$, only marginally deviates from the nominal composition, $Ti_{47}Cu_{38}Zr_{7.5}Fe_{2.5}Sn_2Si_1Ag_2$. In other words, gas atomization did not result in any significant compositional changes. The oxygen content of the powder is 930 ± 25 ppm. After SLM processing, the alloy contains more oxygen (1250 ± 40 ppm) owing to the high affinity of Ti to oxygen.

The diffraction patterns of the powder, a SLM sample and an as-cast rod are displayed in Fig. 1a. Some sharp reflections superimpose on a broad background typical of metallic glasses in the case of the powder. The reflections are identified to result from Ti_2Cu, Ti_3Cu_4 and TiCu [17]. The cooling rate during gas atomization is not high enough to suppress crystallization and as a result, partially crystalline powder is obtained. This is unexpected because the critical casting thickness has been reported to reach 7 mm [17] and gas atomization with its high intrinsic cooling rates should yield fully amorphous powder. In spite of the elevated oxygen content in the powder, no stable or metastable phases with icosahedral order (quasicrystals or the big cube phase) [18,19] precipitate. In contrast, the diffraction patterns of the SLM sample and the as-cast rod only exhibit a broad scattering maximum and appear to be fully glassy. It is noteworthy that the alloy vitrifies during SLM although the cooling rates should be similar to those of gas atomization [20]. The short lifetime of the melt pool [21] seems sufficient to overcome the slight chemical segregation, which accompanies the formation of the present Ti-rich Ti_2Cu phase and to produce a chemically uniform melt. The subsequent cooling, again, proceeds sufficiently fast to warrant vitrification.

All the samples show the typical features of metallic glasses, i.e. a distinct glass transition followed by a supercooled liquid region prior to multiple exothermic events associated with crystallization (Fig. 1a). The glass-transition temperature, T_g, as well as the onset-temperature of crystallization, T_x, are indicated in Fig. 1b. The values of T_g (659 ± 1 K), T_x (707 ± 1 K) and enthalpy of crystallization, ΔH_{cryst} (26 ± 1 J/g) of the first crystallization event are identical within the experimental error for the as-cast rod and the SLM sample. Only the powder is obviously different (T_g = 642± 1 K, T_x = 698 ± 1 K, ΔH_{cryst} = 24 ± 1 J/g) due to its partially crystalline nature. In other words, SLM processing or the elevated oxygen content do not measurably deteriorate the glass-forming ability or the stability of the glass against crystallization.

The relative densities of the specimens (Archimedean) range from 98.5% to 98.7% and the densest specimens were investigated by μ-CT. In the cross-sectional view of Fig. 2a, small pores with a typical diameter of 10–30 μm can be found. Only a few slightly larger defects locate at the edge of the sample. The full μ-CT reconstruction of a SLM sample (inset to Fig. 2b) reveals that the pores are uniformly distributed throughout the sample. From this μ-CT scan the pore size distribution was extracted (Fig. 2b). The vast majority of the pores has diameters between 15 and 35 μm. The relative density evaluated from the μ-CT reconstruction amounts to 99.5%–99.7% which is higher than the values obtained from the Archimedean principle (98.5%–98.7%). Because of the limited resolution of the device small pores (<10 μm) cannot be detected by μ-CT. In addition, small air bubbles can adhere to the rough surface of the SLM samples which may influence the results of the Archimedean measurement and could account for the observed discrepancy.

Fig. 3a compares the true stress-strain curves for two representative samples. The as-cast sample yields at stresses around 2000 MPa and exhibits serrated flow in the plastic stage. The Young's modulus of both samples is E = 100 ± 5 GPa and the as-cast sample fails after a plastic strain of about 1.8%. The SLM samples, however, fractures at lower stress (1690 ± 50 MPa) without any significant plastic deformation. Unlike the as-cast rods, which have a well-defined, relatively smooth fracture plane inclined by 45° with respect to the loading axis (not shown here), the fractured SLM samples appear completely different. Vein-like patterns [22] can be found on both fracture surfaces but one cannot identify a clear fracture plane (inset to Fig. 3a) for the SLM samples. The fracture angle is almost 90° with respect to the loading axis which indicates that the stress state and fracture mode is rather different for the SLM samples. The defects introduced during additive manufacturing seem responsible for the premature failure and the differences

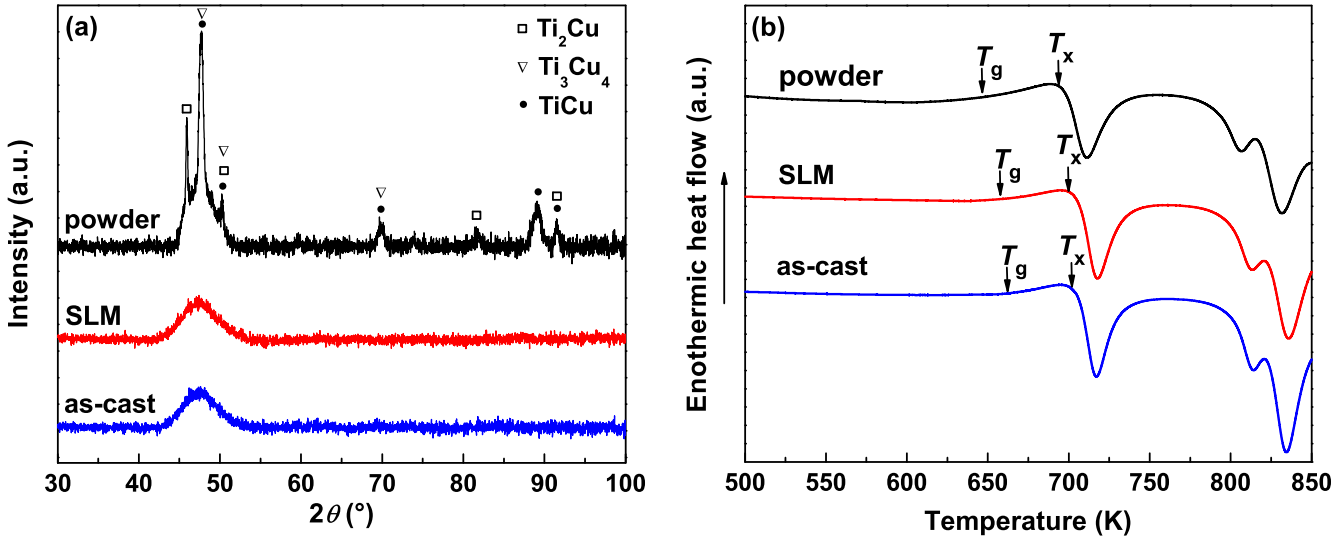

Fig. 1. (a) X-ray diffraction patterns of the $Ti_{47}Cu_{38}Zr_{7.5}Fe_{2.5}Sn_2Si_1Ag_2$ powder, a cylindrical SLM sample and an as-cast rod. Crystalline reflections only appear in the gas-atomized powder. (b) DSC traces of the $Ti_{47}Cu_{38}Zr_{7.5}Fe_{2.5}Sn_2Si_1Ag_2$ powder, a cylindrical SLM sample and an as-cast rod. The glass-transition temperature, T_g and the onset of crystallization, T_x, are marked by arrows.